PHYSICAL REVIEW B **82**, 121405(R) (2010)

Spin-polarized semiconductor induced by magnetic impurities in graphene

Maria Daghofer,[1,2,3,*] Nan Zheng,[1,2,4] and Adriana Moreo[1,2]
[1]*Department of Physics and Astronomy, University of Tennessee, Knoxville, Tennessee 37996-1200, USA*
[2]*Materials Science and Technology Division, ORNL, Oak Ridge, Tennessee 37831-6032, USA*
[3]*IFW Dresden, P.O. Box 27 01 16, D-01171 Dresden, Germany*
[4]*Department of Computer Science, The College of William and Mary, Williamsburg, Virginia 23187, USA*
(Received 23 August 2010; published 10 September 2010)

The effective magnetic coupling between magnetic impurities adsorbed on graphene, which is mediated by the itinerant graphene electrons, and its impact on the electrons' spectral density are studied. The magnetic interaction breaks the symmetry between the sublattices, leading to antiferromagnetic order, and a gap for the itinerant electrons develops. Random doping produces a semiconductor but if all or most of the impurities are localized in the same sublattice the spin degeneracy can be lifted and a spin-polarized semiconductor induced.

DOI: 10.1103/PhysRevB.82.121405 PACS number(s): 73.22.Pr, 71.10.Fd, 72.25.Dc

I. INTRODUCTION AND MODEL

Graphene has been the focus of active research in the last few years due to its peculiar transport properties[1–5] and its potential technological applications. For spintronic devices,[6] where the high electron mobility and tunable electron filling make graphene an interesting candidate, it is important to investigate magnetism and the possibility of spin-polarized conduction electrons. Moreover, it would be desirable to transform graphene from a semimetal into a semiconductor. In the present Rapid Communication, we are going to show that localized magnetic impurities (MIs) provide a way to open a gap.

Density-functional-theory (DFT) calculations suggest that decorating graphene nanoribbons with metal ions can lead to opposite spin polarization in the valence and conduction bands.[7] This property is known as *spin-polarized half-semiconductivity* and it is very desirable for spintronics devices.[8] DFT also predicts that interfaces between Ni or Co layers and graphene or graphite could induce spin polarization[9] because only the majority spin bands of the Co or Ni have an overlap with the graphene bands. We will show that MIs, which do not directly donate spin-polarized electrons to the graphene layer, can nevertheless polarize its electrons in the direction *opposite* to their own spin.

Magnetic impurities in graphene can either arise as effective magnetic moments of nonmagnetic impurities[10,11] or from intrinsically MIs. The feasibility of introducing MIs by embedding transition metal ions has been studied by *ab initio* methods[12,13] and can be achieved using a scanning tunneling microscope.[14] Recently, Kondo physics indicating strong coupling between conduction electrons and MIs has been reported,[11] suggesting that defects indeed offer a route to tune the electronic properties of graphene. Single MIs lead to spin-polarized midgap states[15] and have been suggested to act as a spin valve.[16] The magnetic coupling between impurities is expected to be ferromagnetic (FM) [antiferromagnetic (AF)] for impurities in the same (different) sublattices.[10,13,17–20] We are going to discuss the ordering of MIs mediated by the electrons and the spectral properties of these electrons, which then move in a background of ordered MIs.

The simplest description of graphene is a tight-binding Hamiltonian given by the hopping of the carbon-π_z electrons between nearest neighbor (NN) sites of a honeycomb lattice (see Fig. 1). The symmetry between the two C atoms in the unit cell leads to the Dirac cones making up the Fermi surface (FS), located at the points K_1 and K_2 [see inset in Fig. 2(a)]. If this symmetry is broken, e.g., by an energy difference between the sublattices, a gap can be opened, and dispersive edge states within the gap were proposed to arise at domain boundaries[21] or edges[22] of areas with broken sublattice symmetry. The sublattices could be made inequivalent by a substrate with a matching lattice constant[23] or via nonmagnetic impurities but only if they mostly occupy sites in only one sublattice.[21] As it will be shown in this Rapid Communication, the situation is different—and possibly simpler—for MIs. Due to their AF coupling, they turn out to be oriented in opposite directions in the two sublattices and an electron that gains magnetic energy in one sublattice,

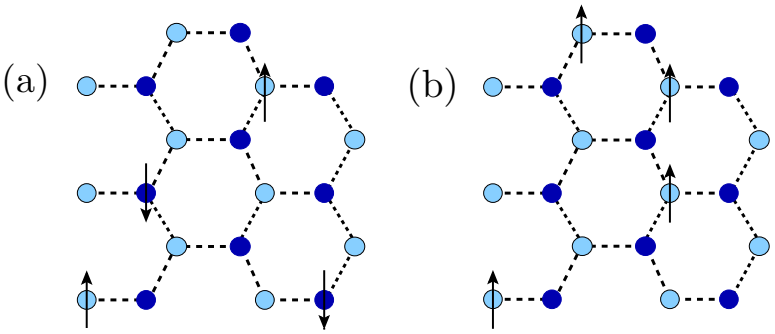

FIG. 1. (Color online) Cartoon of MIs on graphene. Light (dark) circles indicate C atoms in sublattice A (B). Lines show the NN connections, where the electrons hop. Arrows illustrate MIs located on top of C atoms, which are either (a) distributed equally over both sublattices and AF ordered, or (b) located only in sublattice A and FM ordered.

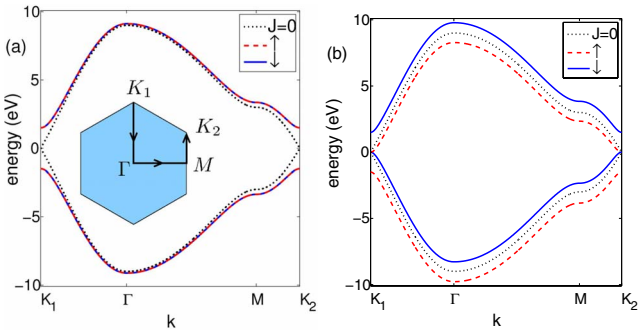

FIG. 2. (Color online) Dispersion for electrons that couple with $J=1.5$ eV to perfectly ordered MI spins. (a) Equation (3) for AF ordered MIs on all sites. The curves for up and down spins lie on top of each other. (b) Equation (4) for MIs on one sublattice only; all impurity spins are parallel and up. The dotted line in each panel gives the bands for $J=0$. The inset in (a) shows the path through the first Brillouin zone.

looses it in the other. Thus, the sublattices are inequivalent for either spin projection and both are expected to develop a gap regardless of the impurity distribution. If, however, MIs or a magnetic substrate can be engineered to interact predominantly with only one sublattice, electrons at the top (bottom) of the valence (conduction) band will be shown to be spin polarized.

The itinerant electrons interacting with randomly located MIs—represented by an onsite magnetic moment $\mathbf{S_I}$—[24]are described by the Hamiltonian

$$H = -t\sum_{\langle \mathbf{i},\mathbf{j}\rangle,\sigma}(c^{\dagger}_{\mathbf{i},\sigma}c_{\mathbf{j},\sigma}+\text{H.c.}) - 2J\sum_{\mathbf{I}}\mathbf{s_I}\cdot\mathbf{S_I}, \qquad (1)$$

where $c^{\dagger}_{\mathbf{i},\sigma}$ creates an electron with spin σ, $\langle \mathbf{i},\mathbf{j}\rangle$ are NN sites in the honeycomb lattice, J gives the strength of the magnetic interaction between the impurities and the electrons, and the spin of the electrons is given by $\mathbf{s_I}=\Sigma_{\alpha,\beta}c^{\dagger}_{\mathbf{I},\alpha}\sigma_{\alpha,\beta}c_{\mathbf{I},\beta}$. The system is half-filled, i.e., one electron per site, and $t=3$ eV.[25,27] To simplify the calculations and to avoid the "sign problem" in the Monte Carlo (MC) simulations, we treat the MI spins as classical vectors. This approximation is valid for large impurity spins $S\gtrsim 1$, as is expected to hold for transition metal ions adsorbed on graphene,[26] and the localized spins then simply act as a spin-dependent impurity potential on the itinerant electrons. The magnitude of the spin is absorbed into the coupling constant J, giving $2J\approx 3$ eV.[28] Coulomb repulsion between the conduction electrons is neglected, as has been found appropriate in many physical situations.[17,29] Since our lattices are considerably larger than the distances between impurities, finite-size effects are not expected to be severe.[20]

II. RESULTS AND DISCUSSION

For $J=0$, the Hamiltonian can be easily diagonalized and the band structure along the path K_1-Γ-M-K_2 is shown as a dotted line in Fig. 2. The two C atoms of the basis lead to two states per momentum $\mathbf{k}$ with energies

$$\pm\epsilon(\mathbf{k}) = \pm\sqrt{1+4\cos\frac{k_y}{2}\cos(\sqrt{3}k_x/2)+4\cos^2\frac{k_y}{2}}. \qquad (2)$$

The momenta $\mathbf{k}=(k_x,k_y)$ allowed for $N_x\times N_y$ are $k_x=4\pi n_x/(N_x a\sqrt{3})$ with $n_x=0,\pm 1,\ldots,N_x/2$ and $k_y=4\pi n_y/N_y$ with $n_y=0,\pm 1,\ldots,N_y/3$ (Ref. 30) and the two bands are degenerate at the points K_1 and K_2.[27]

We can also diagonalize Eq. (1) for one MI per lattice site with all the MIs in sublattice A (B) parallel to $\hat{\mathbf{z}}$ ($-\hat{\mathbf{z}}$). The spin-degenerate bands are given by

$$E(\mathbf{k}) = \pm\sqrt{J^2+\epsilon(\mathbf{k})^2}. \qquad (3)$$

Since nonmagnetic impurities need to be concentrated on one sublattice to induce a gap, the resulting gap of size $2J$ [see Fig. 2(a)] suggests that MIs might provide a simpler way to turn graphene into a semiconductor.

A different situation arises if all MIs are in one sublattice and parallel to $\hat{\mathbf{z}}$. The energy then depends on the spin and for the spin parallel (antiparallel) to $\hat{\mathbf{z}}$, denoted by "up" ("down"), we find

$$E^{\uparrow}(\mathbf{k}) = -\frac{J}{2}\pm\sqrt{\frac{J^2}{4}+\epsilon(\mathbf{k})^2}, \quad E^{\downarrow}(\mathbf{k}) = \frac{J}{2}\pm\sqrt{\frac{J^2}{4}+\epsilon(\mathbf{k})^2}. \qquad (4)$$

The resulting bands are shown in Fig. 2(b) and not surprisingly, the electrons parallel to the localized spins are energetically favored. But as one band for each spin direction lies below the chemical potential, there is no net polarization of the itinerant electrons even though all localized spins are perfectly FM. This follows from the degeneracy induced by the two-atom basis and it means that the electrons in the "clean" sublattice are polarized in the opposite direction so that the contributions from the electrons in the two sublattices exactly cancel. While there is thus no ferrimagnetism and no net spin polarization of the itinerant electrons, the band structure in Fig. 2(b) nevertheless has energy regions with well developed majority spins: in particular, the electrons *directly below and above the Fermi level are polarized*.

As long as J is not too large ($J\lesssim 2t$), the results remain similar even if not all sites of the (sub-) lattice have a MI, and the ordered AF leads to dispersive bands instead of localized impurity states. To show this, the Hamiltonian given by Eq. (1) was diagonalized numerically for lattices with $N_x\times N_y=72\times 72=5184$ sites containing $N_{\text{imp}}=864=72^2/6$ randomly distributed impurities. The impurity spins were set into a magnetically ordered state, where all spins in sublattice A (B) are parallel (antiparallel) to $\hat{\mathbf{z}}$. The spectral function $A(\mathbf{k},\omega)$ is shown in Fig. 3(a) for equal numbers of MIs in both sublattices. (Notice that the bands for spin up and down are here degenerate.) Similar to the case of nonmagnetic impurities,[21] the most prominent change is that the gap is renormalized from $2J$ to $2c_{\text{imp}}J$ for an impurity concentration $c_{\text{imp}}=N_{\text{imp}}/(N_xN_y)$. This can be seen by comparing $A(\mathbf{k},\omega)$ and the white line given by Eq. (3) with a renormalized $\hat{J}=c_{\text{imp}}J$. The inset shows the resulting gap of $2\hat{J}=2c_{\text{imp}}J=0.5$ eV. Doping with MIs thus turns graphene into a semiconductor via the AF ordering of both the MIs and the graphene electrons.

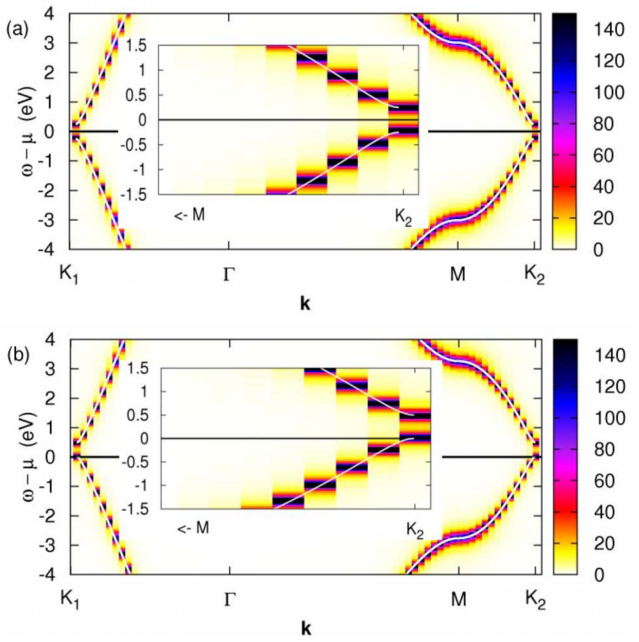

FIG. 3. (Color online) Spectral density for down electrons. (a) Impurity spins are distributed in both sublattices; the spectral density for up electrons looks identical. (b) Impurities are in sublattice A only and oriented along $+\mathbf{z}$, i.e., the down electrons are antiparallel. $A(\mathbf{k},\omega)$ for up electrons is the mirror image about the chemical potential μ, see Fig. 2(b). The white lines indicate the bands of translationally invariant systems described by (a) Eq. (3) and a renormalized $\hat{J}=c_{\mathrm{imp}}J$ and (b) Eq. (4) and $\hat{J}=2c_{\mathrm{imp}}J$. Parameters are: $N_x\times N_y=72\times 72$, $864=72^2/6$ impurities, and $J=1.5$ eV$=t/2$.

In Fig. 3(b), we present the band dispersion for the "down" electrons (i.e., antiparallel to the impurity spins) for 864 MIs randomly distributed in one of the sublattices. Since the sublattice containing the MIs effectively has a doubled impurity concentration of $c_{\mathrm{eff}}=2c_{\mathrm{imp}}=N_{\mathrm{imp}}/(N_xN_y/2)$, the renormalized gap resulting from Eq. (4) is given by $\hat{J}=2c_{\mathrm{imp}}J=0.5$ eV, the same as for impurities in both sublattices. The gap is thus independent of the percentage of impurities found in each sublattice. The inset of Fig. 3(b) reveals that the gap now opens above the chemical potential μ, while the gap for spin up (not shown) is below μ. (The up and down bands are mirror images about μ.) When all MIs are in one sublattice, the highest occupied states are thus clearly spin polarized, leading to the *spin-polarized half-semiconductor* described in Ref. 7.

If the MI distribution is not perfect and a fraction $p<1$ of the MIs are in one sublattice and $1-p>0$ in the other, the exact degeneracy of up and down states at K_1 and K_2 is lifted and a gap of order $4(1-p)Jc_{\mathrm{imp}}$ opens between the highest occupied down states and the lowest empty up states. The gaps for each spin direction bands remain asymmetric about μ as long as $p\gg 0.5$ (or $p\ll 0.5$), thus preserving the spin polarization for a reduced energy window $2(2p-1)Jc_{\mathrm{imp}}$. Again, the translationally invariant and the dilute systems behave similarly: The ordered state of the MIs preserves coherent electron motion in highly dispersive bands (albeit with a finite mass) and we only find localized impurity states with small dispersion for very large $J\gtrsim 2t$.

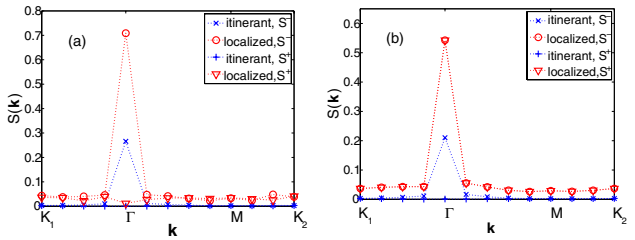

FIG. 4. (Color online) Spin structure factor for momenta along the path shown in the inset of Fig. 2(a). Symmetric (S^+) and antisymmetric (S^-) components indicating FM and AF order are shown for the localized impurity spins as well as for the itinerant electrons for (a) each sublattice containing exactly half of the randomly distributed impurities and (b) all the impurities randomly distributed in the A sublattice. $J=6$ eV, $\beta t=100$, corresponding to $T\approx 300$ K, $N_x=N_y=12$, and $N_{\mathrm{imp}}=24=12^2/6$. The data were averaged over (a) six and (b) ten impurity configurations.

After discussing electrons interacting with perfectly ordered spins, we present results of unbiased MC simulations. They were performed on the angles $\theta_{\mathbf{I}}$ and $\phi_{\mathbf{I}}$ defining the orientation of the MI spins in Eq. (1); the probability of a spin configuration is obtained by diagonalizing the effective electronic Hamiltonian.[31] Studies for lattice sizes up to 18×18, for $150<T<1500$ K, for various values of J, and for different impurity concentrations showed indications of long-range magnetic order.

Each momentum $\mathbf{k}$ has a spin-structure factor $S_A(\mathbf{k})$ for sublattice A and $S_B(\mathbf{k})$ for sublattice B. They indicate the magnetic order within the sublattice with a signal at the Γ point ($\mathbf{k}=0$) signifying FM order between all spins in the same sublattice. S_A and S_B can be combined into symmetric ($S^+=S_A+S_B$) and antisymmetric ($S^-=S_A-S_B$) combinations, which give information about the order between the sublattices: if the spins in sublattice A and B are parallel (antiparallel), this is revealed by a signal in S^+ (S^-). In Fig. 4, S^+ and S^- are shown as a function of the momentum. One sees clear peaks at Γ, indicating that the itinerant electrons mediate order between the localized spins and that all spins within a sublattice are FM. For MIs located in both sublattices, the signal is in the S^- channel [see Fig. 4(a)], which shows AF order between the sublattices.

If sublattice B is free from MIs, it does not contribute to the impurity-spin structure factor, leading to $S^+=S^-=S_A$, and the signal at Γ indicates FM order within the MI-doped sublattice [see Fig. 4(b)]. The MC simulations thus clearly demonstrate FM order within sublattices and AF order between them, justifying the choice of the ordered configurations discussed above.[32] The itinerant electrons always give a peak at Γ in the AF S^- channel, regardless of the MI distribution. Since there is *no* signal in the symmetric channel S^+ (we verified that this holds for all momenta), ferrimagnetism can be ruled out and the itinerant electrons do not develop a net magnetic moment, as discussed previously for the perfectly ordered MI spins.

For small lattices, the few available momenta mean a large finite-size energy spacing of the kinetic energy and an asymmetric gap, as seen in Figs. 2(b) and 3(b) does then not show up very clearly. The smaller lattices accessible to MC

require thus the use of larger values of $J \gtrsim t$ to allow us to analyze $A(\mathbf{k}, \omega)$. Where the analysis is possible, the MC data agree with the ground-state results. For MIs in only one sublattice, the spin polarization is reduced by finite-temperature fluctuations but the states around the FS remain predominantly down ($\omega \lesssim \mu$) and up ($\omega \gtrsim \mu$). The unbiased MC calculations thus corroborate the results for magnetically ordered configurations.

III. CONCLUSIONS

We have discussed itinerant electrons in graphene interacting with MIs localized on top of the C atoms. We found that the electrons always develop AF correlations and that a gap opens for both spin projections, regardless of the distribution of the MIs between the two sublattices. Domain boundaries or edges of nanoribbons[7,21,22] are expected to support edge states within the gap. For MIs randomly distributed between the sublattices, we find a standard semiconductor with a gap that can be tuned by adjusting the impurity concentration. While the carriers acquire a mass, their dispersion remains almost that of clean graphene. If all or most MIs are in one sublattice[33] the highest occupied (lowest unoccupied) states are spin polarized antiparallel (parallel) to the MIs, giving rise to a spin-polarized semiconductor that could be useful to inject polarized electrons into devices. We find that MIs with large spin located on top of C atoms are the most likely candidates to produce these effects.

ACKNOWLEDGMENTS

This work was supported by the National Science Foundation under Grant No. DMR-0706020, the Division of Materials Sciences and Engineering, Office of Basic Energy Sciences, U.S. DOE, and the DFG under the Emmy-Noether program.

*m.daghofer@ifw-dresden.de

[1] K. Novoselov *et al.*, Nature (London) **438**, 197 (2005).
[2] K. Novoselov *et al.*, Nat. Phys. **2**, 177 (2006).
[3] J. Tworzydło, B. Trauzettel, M. Titov, A. Rycerz, and C. W. J. Beenakker, Phys. Rev. Lett. **96**, 246802 (2006).
[4] S. V. Morozov, K. S. Novoselov, M. I. Katsnelson, F. Schedin, L. A. Ponomarenko, D. Jiang, and A. K. Geim, Phys. Rev. Lett. **97**, 016801 (2006).
[5] A. H. Castro Neto *et al.*, Rev. Mod. Phys. **81**, 109 (2009).
[6] I. Žutić, J. Fabian, and S. Das Sarma, Rev. Mod. Phys. **76**, 323 (2004).
[7] F. Cervantes-Sodi, G. Csányi, S. Piscanec, and A. C. Ferrari, Phys. Rev. B **77**, 165427 (2008).
[8] V. Prigodin *et al.*, Adv. Mater. **14**, 1230 (2002).
[9] V. M. Karpan, P. A. Khomyakov, A. A. Starikov, G. Giovannetti, M. Zwierzycki, M. Talanana, G. Brocks, J. van den Brink, and P. J. Kelly, Phys. Rev. B **78**, 195419 (2008).
[10] H. Kumazaki and D. S. Hirashima, J. Phys. Soc. Jpn. **75**, 053707 (2006); **76**, 064713 (2007); J. Magn. Magn. Mater. **310**, 2256 (2007).
[11] J. Chen, W. Cullen, E. Williams, and M. Fuhrer, arXiv:1004.3373 (unpublished).
[12] A. V. Krasheninnikov, P. O. Lehtinen, A. S. Foster, P. Pyykkö, and R. M. Nieminen, Phys. Rev. Lett. **102**, 126807 (2009).
[13] E. J. G. Santos, D. Sánchez-Portal, and A. Ayuela, Phys. Rev. B **81**, 125433 (2010).
[14] B. Uchoa, V. N. Kotov, N. M. R. Peres, and A. H. Castro Neto, Phys. Rev. Lett. **101**, 026805 (2008); D. M. Eigler and E. K. Schweizer, Nature (London) **344**, 524 (1990).
[15] S. Casolo, O. M. Løvvik, R. Martinazzo, and G. F. Tantardini, J. Chem. Phys. **130**, 054704 (2009).
[16] P. S. Cornaglia, G. Usaj, and C. A. Balseiro, Phys. Rev. Lett. **102**, 046801 (2009).
[17] L. Brey, H. A. Fertig, and S. Das Sarma, Phys. Rev. Lett. **99**, 116802 (2007).
[18] O. V. Yazyev and L. Helm, Phys. Rev. B **75**, 125408 (2007).
[19] S. Saremi and P. A. Lee, Phys. Rev. B **75**, 165110 (2007); V. K. Dugaev, V. I. Litvinov, and J. Barnaś, *ibid.* **74**, 224438 (2006).
[20] V. V. Mkhitaryan, E. G. Mishchenko, M. E. Raikh, and L. I. Glazman, Phys. Rev. B **80**, 205416 (2009).
[21] V. Cheainov, O. Syljuåsen, B. Altshuler, and V. Fal'ko, EPL **89**, 56003 (2010).
[22] W. Yao, S. A. Yang, and Q. Niu, Phys. Rev. Lett. **102**, 096801 (2009).
[23] G. Giovannetti, P. A. Khomyakov, G. Brocks, P. J. Kelly, and J. van den Brink, Phys. Rev. B **76**, 073103 (2007).
[24] Several locations for MIs have been considered in the literature. We are treating MIs that interact mostly with the electrons at one particular lattice site. This corresponds, e.g., to substitutional impurities or moments induced by vacancies (Refs. 17, 18, 25, and 26).
[25] M. A. H. Vozmediano, M. P. López-Sancho, T. Stauber, and F. Guinea, Phys. Rev. B **72**, 155121 (2005).
[26] D. M. Duffy and J. A. Blackman, Phys. Rev. B **58**, 7443 (1998).
[27] R. Saito, G. Dresselhaus, and M. S. Dresselhaus, *Physical Properties of Carbon Nanotubes* (Imperial College Press, London, 1998).
[28] K. Sengupta and G. Baskaran, Phys. Rev. B **77**, 045417 (2008).
[29] S. Das Sarma, E. H. Hwang, and W.-K. Tse, Phys. Rev. B **75**, 121406(R) (2007); M. Polini *et al.*, Solid State Commun. **143**, 58 (2007); J. González, F. Guinea, and M. Vozmediano, Nucl. Phys. B **424**, 595 (1994); H. P. Dahal, Y. N. Joglekar, K. S. Bedell, and A. V. Balatsky, Phys. Rev. B **74**, 233405 (2006).
[30] A. Ceulemans, L. F. Chibotaru, S. A. Bovin, and P. W. Fowler, J. Chem. Phys. **112**, 4271 (2000).
[31] E. Dagotto, T. Hotta, and A. Moreo, Phys. Rep. **344**, 1 (2001).
[32] MC snapshots also corroborate this magnetic order.
[33] This distribution is needed to get a gap with non-MIs (Ref. 21).